35th Annual International Conference of the IEEE EMBS
Osaka, Japan, 3 - 7 July, 2013

Estimation of Glance from EEG for Cursor Control

Tele Tan, Jan Philipp Hakenberg and Cuntai Guan

Abstract – **The variations in the electrooculogram (EOG) caused by eye motion are roughly proportional to the instantaneous horizontal and vertical glance angle. This linear correlation is exploited in systems using EOG to control software, and hardware such as artificial limbs, or wheelchairs. In these approaches, the drift in the electronics is commonly compensated by applying a high-pass filter. Consequently, the remaining EOG signal contains only blinks and rapid eye movement. However, repeating these eye gestures voluntarily is exhausting. This paper presents an algorithm that estimates the instantaneous glance of a subject from EEG signals. The subject is seated in front of a computer screen to control an application by glance. Because the visual field of interest, in this setting, is the limited area of the monitor, we can compensate the error in the glance estimate by detecting outliers. Because no high-pass filter is applied to the data, the user controls the applications by eye glance, which is comfortable and can be performed over extended periods of time. The numerical evaluation of the experiments with 12 volunteers, and video recordings of EOG controlled applications demonstrate the accuracy of our algorithm.**

I. INTRODUCTION

The front and the back of the human eye sustain an electric potential difference. The potentials propagate to the cheeks, forehead, and scalp, where electrooculogram (EOG), or electroencephalogram (EEG) electrodes can pick them up. A reorientation of the eyes generally causes a change in the voltages measured by the electrodes.

Whereas the signal patterns originating from eye movement are undesired in applications that monitor brain activity, the patterns constitute a reliable means of control in an EOG based human-machine interface. A person without correct limb and facial muscular control might still have the ability to gesture through eye movement and blinks. Diseases such as amyotrophic lateral sclerosis, or certain forms of quadriplegic clinical conditions (spinal cord injury, locked-in syndrome) render patients with as little forms of expression as blinking and orienting the eyes. Automating the interpretation of these gestures can lead to a more autonomous lifestyle and increased quality of life [1].

Researchers have been particularly successful at detecting eye blinks in the EOG, and classifying oscillatory eye movements. Consequently, these eye gestures would operate a wheelchair [1], a robot [2], or software for spelling words, and express needs in a home environment [3]. In the future, psychological research, gaming electronics, consumer electronics, and the long term examination of eye movements might result in more applications [4]. Compared to video-based eye trackers, EOG is independent of lighting conditions and also works when the eye lids are closed [5]. Besides, EOG is used to remove ocular artifacts from EEG to unveil brain activity [6]. The technique presented in our paper does not categorize as brain computer interface as the control is not based on the classification of brain activity.

Common within the literature on EOG-based control is the application of a high-pass filter, with cutoff at a frequency between 0.05 and 0.2 Hz. The high-pass filter removes the long-term drift inherent in all channels that are connected to the scalp [7]. Over short periods of time, typically less than ten seconds, the drift is negligible given that the subject is at rest. During this phase, the variation in EOG is nearly co-linear to the glance angle within the customary field of view [8], thus linear regression techniques can reliably transforms EOG to glance direction. However, since the EOG-based control is required to operate for extended periods of time, researchers have relied on the classification of oscillatory eye movements from the high-pass filtered data. One exception is [2], who performs periodic recalibrations: To reset the positional control, the user ”fixates on a direct forward gaze for approximately 1/2 second, then blinks.” Another approach is presented in [9], that fits the measured velocity profile of the EEG during a saccade to the average velocity profile during a standard saccade in order to integrate the eye rate over time to the glance direction.

Our new approach is motivated by two observations:

- The majority of EOG-controlled applications are displayed on a computer screen to provide feedback with the shortest amount of delay possible. When the glance is falsely estimated to lie outside of the screen area, a simple translation can account for the offset. Drift is corrected on the fly.
- Activities such as reading and watching a movie are comfortably performed over extended periods of time, during which the glance targets the changing region of interest, while blinks occur infrequently and involuntarily. Any EOG-based application that creates the incentive for the same behavioural pattern is likely to have low fatiguing effect. Until now, most applications are based on voluntary blinks and oscillation of glance.

The paper is organized as follows: We advocate the use of a linear model to estimate eye orientation from raw EEG data. No filtering is required. The subject- and session-specific model is obtained from a short calibration procedure. In order to accurately estimate the glance over extended periods of time on a computer screen, we introduce

T. Tan and J.P. Hakenberg are with Curtin University, GPO Box U1987, Perth, Western Australia (phone: +61 8 92661207; fax: +61 8 92662681; e-mail: t.tan@curtin.edu.au).

C. Guan is with Institute for Infocomm Research, 1 Fusionpolis Way, Singapore 138632 (e-mail: ctguan@i2r.a-star.edu.sgdu).

a drift compensation that translates outliers back onto the screen. A simple computation reveals that our algorithm is potentially invariant under arbitrary shift of baselines. Finally, we provide empirical data supporting the performance of the eye glance estimation and report on two conventional applications that were developed using this approach.

II. METHOD

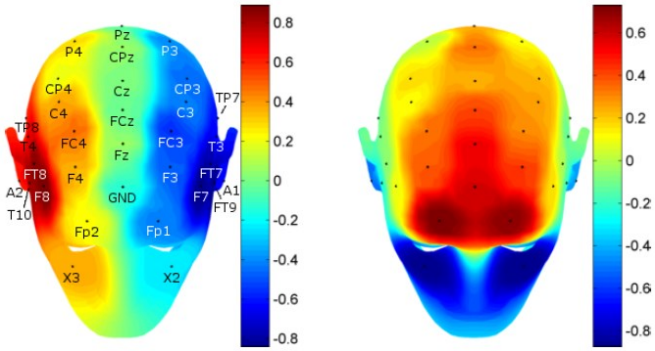

Fig. 1: Linear correlation coefficients of channel measurements with horizontal (left) and vertical (right) glance direction averaged for 12 subjects as presented in [10]. The reference electrode is Oz at the back of the head. Values of ±1 would indicate a perfect linear correlation. The black dots indicate the location of electrodes between which the values are interpolated.

A. Model

Voltage gradients measured from skin around the eyes exhibit a nearly perfect linear correlation with the glance ranging within ±45◦ for left-right and within ±30◦ for up-down direction [8]. For electrodes further away, located on the scalp, the correlation coefficients were studied in [10] and are reproduced in Figure 1. For instance, electrodes on the temples correlate significantly with the left-right glance, whereas channels located along the centreline of the scalp exhibit a significant correlation with the up-down glance. Our model to estimate the glance from EEG exploits the cumulative linear correlation with the vertical and horizontal glance direction of all connected channels.

We assume the EEG amplifier provides the number of n channels, which are referenced to a ground electrode. For each channel, $i = 1, 2, \dots, n$, the measured EEG signal m_i is the sum of the effect of the glance g_i, and a remaining signal component c_i that is composed of (1) a channel specific, drifting baseline, (2) potential fluctuation induced by brain activity, as well as 3) noise. The contributions of (2) and (3) above are of significantly lower amplitude than the glance g_i and have zero mean. We write $m_i = g_i + c_i$ for $i = 1, 2, \dots, n$.

A computer screen is placed in front of the subject in close proximity given that the glance can still be comfortably directed into all corners of the screen. Let $p = (x, y)$ denote the normalised coordinate on the screen (i.e. $-1 \leq x, y \geq 1$). The contribution of the glance g_i on channel $i = 1, 2, \dots, n$ is modelled as $g_i(p) = \beta_i^x \cdot x + \beta_i^y \cdot y$ where β_i^x, β_i^y are related to the coefficients shown in Figure 1.

B. Calibration

During the calibration procedure of duration T, the subject is required to visually trace a moving cue at coordinate $p(t) = (x(t), y(t))$ on the screen while keeping the head as still as possible. Subsequent to the calibration procedure, the system tolerates turning and tilting of the head quite successfully due to the way drift is handled (see Section III.C). Because of linearity, we express the correlation of the measurements m_i and the glance direction (x, y) at time t simply by the matrix multiplication

$$(m_1 \quad m_2 \quad \cdots \quad m_n \quad 1) \begin{pmatrix} \propto_1^x & \propto_1^y \\ \propto_2^x & \propto_2^y \\ \vdots & \vdots \\ \propto_n^x & \propto_n^y \\ \propto_0^x & \propto_0^y \end{pmatrix} = (x \quad y) \qquad (1)$$

The EEG collected during the calibration procedure from $t = 0, \dots, T$, and the coordinates of the cue up-sampled to the rate of the EEG compile into an over-determined system of linear equations. The unknowns $\propto_i^x, \propto_i^y$ for $i = 0, 1, 2, \dots, n$ are solved for by minimizing the squared error in Equation (1). The purpose of the coefficients $\propto_0^x, \propto_0^y$ is to compensate for the baseline offset in all channels. Figure 2 shows the calibration procedure at different points in time.

The synchronization of the EEG m_i with the cue position p on the screen is crucial in solving Equation (1). The common practice is to send trigger pulses to the amplifier via serial port messaging. However, there remains a bias that depends on the response rate of different graphics systems. So instead, we mount a photodiode circuit in front of the display to determine the lag between vision and EEG. The circuit consists of a photodiode and a resistor, and feeds directly into one of the spare channels of the amplifier. Periodic flashes on the display beneath the photodiode result in pulses of 100μV amplitude, and provide means of synchronization. The photodiode circuit is not required after calibration, as simply the most recent EEG available is used to estimate the glance direction.

C. Algorithm

Subsequent to the calibration procedure, we assume that the position $p = (x, y)$ of the glance on the monitor is unknown. However, having solved the linear system defined by Equation (1), the coefficients $\propto_i^x, \propto_i^y$ for $i = 0, 1, 2, \dots, n$ are at hand to obtain an estimate $\hat{p} = (\hat{x}, \hat{y})$ using the most recent EEG data, m_i.

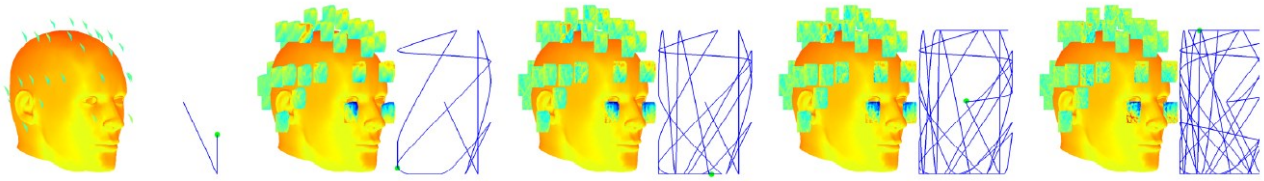

Fig. 2: The cascade visualizes the accumulation of EEG at intervals of 15 seconds as the eyes track the cue that moves along the curve. At each location of the 36 electrodes the voltage is mapped within a square domain at the coordinate corresponding to the cue position.

We simply evaluate

$$(\hat{x} \quad \hat{y}) = (m_1 \quad m_2 \quad \cdots \quad m_n \quad 1)\begin{pmatrix} \propto_1^x & \propto_1^y \\ \propto_2^x & \propto_2^y \\ \vdots & \vdots \\ \propto_n^x & \propto_n^y \\ \propto_0^x & \propto_0^y \end{pmatrix} \qquad (2)$$

Since the signals induced by brain activity as well as the noise are assumed to have zero mean, these contributions are conveniently annihilated by averaging the results of Equation (2) for measurements m_i of the most recent 0.1 sec.

As discussed in [11], the measurements m_i might be subject to drift in the baselines. Consequently, the estimated position $\hat{p}$ is likely to be offset to the actual glance position after a short period of time. We make the assumption that the subject's glance is directed to a point on the computer screen, thus, the estimated position should not be located outside the screen. As soon as Equation (2) yields a coordinate $\hat{x}, \hat{y}$ outside the coordinate area of the screen (i.e. $-1 \leq \hat{x}, \hat{y} \leq 1$), we introduce a correction by translating each coordinate back into the valid area with the minimum shift necessary. This corrective term is applied to subsequent estimations until the condition $-1 \leq \hat{x}, \hat{y} \leq 1$ is violated again.

The horizontal and vertical correction mechanisms are independent and identical, thus we only describe the compensation that corrects the horizontal glance estimation: We introduce a variable q^x to represent the offset of a window of view along the x-axis. Initially, we set $q^x = 0$. Instead of $\hat{x}$, we define $\widehat{x'} = \hat{x} - q^x$ to be the estimated glance position on the screen. If during the process $\widehat{x'}$ lies outside the screen, we simply update q^x. Specifically, if $\widehat{x'} = \hat{x} - q^x < -1$, we redefine $\widehat{x'} = \hat{x} + 1$. On the other hand, if $\widehat{x'} = \hat{x} - q^x > 1$, we update $\widehat{x'} = \hat{x} - 1$. With the modified value q^x the estimation $\widehat{x'} = \hat{x} - q^x$ is guaranteed to be within the bounds of the screen coordinate system [-1, 1]. The final glance estimate is defined as $\widehat{p'} = (\widehat{x'}, \widehat{y'})$.

Figure 3 shows an example how $\hat{x}$ and $\widehat{x'}$ might evolve in practice.

D. Analysis

There are different circumstances that generally lead to a deterioration of the approximation Equation (2); turning of the head or drift in the electrodes. However, our experiments suggest that all of these artefacts can be compensated using the strategy above. In fact, a simple computation reveals that adding constant offsets δ_i to the measurements m_i for $i = 0, 1, 2, \ldots, n$ can be compensated by this algorithm. Again, we demonstrate this only for the x-axis:

$$\propto_0^x + \sum_{i=1}^{n} (m_i + \delta_i)\alpha_i^x = \propto_0^x + \sum_{i=1}^{n} m_i\alpha_i^x + \sum_{i=1}^{n} \delta_i\alpha_i^x = \hat{x} + c \qquad (3)$$

and $\widehat{x'} = \hat{x} + c - q^x$. By allowing for $q^x = c$, then $\widehat{x'} = \hat{x} + c - c = \hat{x}$. Thus, adding constant offsets δ_i to m_i do not necessarily affect the estimation. The offsets δ_i represent the alterations in the baselines due to drift.

III. EXPERIMENTAL RESULTS

A. Subjects and Materials

Twelve subjects aged between 18 and 45 participated in the experiments (Curtin University Ethics Reference SMEC-18-10). Each subject is seated in front of a 22 inch monitor with a distance of 60 cm between forehead and screen. The screen is 47.3 cm wide and 29.7 cm high. Thus, the left-right glance angle ranges between ±21.5°, and the up-down glance angle is between ±13.9°.

To acquire the EEG, we use the 40 channel monopolar digital amplifier NuAmps of which n = 36 channels are effectively connected to the subject. Optionally, two additional EOG electrodes labelled X2 and X3 are placed 2cm below the left and right eye respectively. The amplifier links to the computer via USB. The measurements m_i for $i = 0, 1, 2, \ldots, n$ are transmitted in packets covering time intervals of 0.2 sec, i.e. data packets are received by the controlling computer at a rate of 5 Hz. There is an additional delay of about 0.16 sec until the software that subscribed to the amplifier is notified that data is available.

B. Numerical Evaluation

During calibration, each subject traces a moving cue with coordinates $p(t)$ on the screen over a period of T = 2 minutes while holding the head still. The collected EEG data m_i for $i = 1, 2, \ldots, n$ is used to obtain the coefficients $\propto_i^x, \propto_i^y$ for $i = 0, 1, 2, \ldots, n$ that minimize the squared error in Equation (1). Shortly afterwards, the subject traces the moving cue $p(t)$ again. The EEG data m_i from the second pass together with the coefficients $\propto_i^x, \propto_i^y$ are used to simulate the performance of the algorithm in Section III-C. The output of the algorithm is the estimated target of glance $\widehat{p'}(t)$ in screen coordinates.

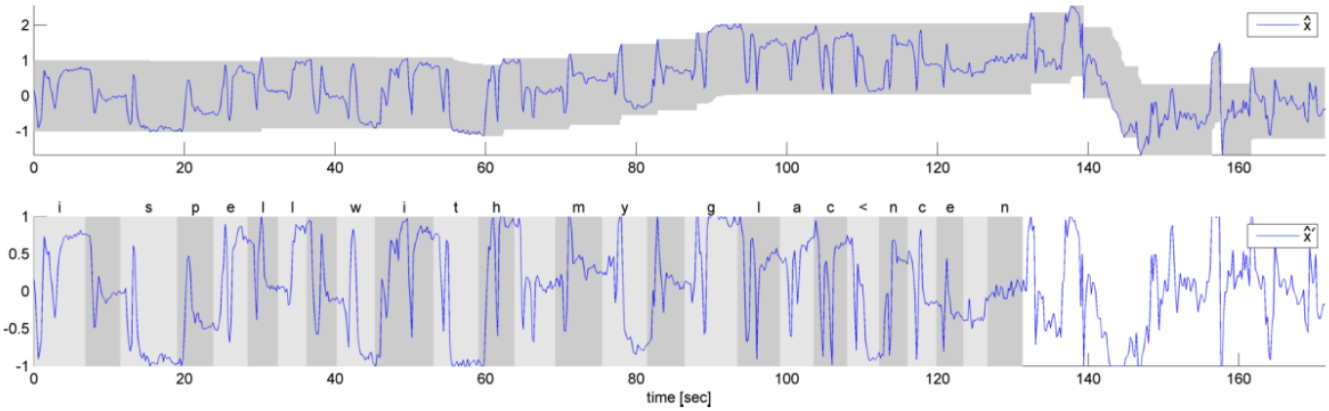

Fig. 3: Glance estimation $\hat{x}$ over a period of 3 minutes (top), and mapped to the interval [±1, 1] results in the final glance estimation $\widehat{x'}$ (bottom)

TABLE 1
VARIANCE OF ESTIMATION ERROR IN [cm^2]

	using X2, X3		without X2, X3	
subject id j	left-right	up-down	left-right	up-down
1	8.265	9.348	8.696	13.215
2	19.261	13.146	22.627	28.866
3	16.146	14.425	16.792	27.840
4	4.231	9.750	5.288	20.281
5	7.065	11.548	7.453	22.460
6	5.562	11.909	5.886	19.723
7	13.040	14.101	14.057	28.596
8	9.259	10.648	11.157	33.778
9	2.174	8.430	2.105	15.958
10	10.108	12.091	12.231	24.787
11	13.205	13.616	15.053	27.776
12	16.430	14.260	17.373	29.466
average	10.395	11.939	11.560	24.396

We scale the difference $d(t) = p(t) - \widehat{p'}(t) = \left(d^x(t), d^y(t)\right)$ according to the actual dimensions of the monitor to formulate the error in [cm] as

$$e(t) = \left(23.65 \cdot d^x(t), 14.85 \cdot d^y(t)\right) \qquad (4)$$

The variance of the estimated error for all 12 subjects is listed in Table 1. The correlation between horizontal and vertical approximation quality is significant. The standard deviation of the average error is less than 3.5 cm in each coordinate, which equivalents to 3.4 degrees of arc. The accuracy of glance estimation using traditional EOG equipment (six electrodes closely placed around the eyes) is stated for comparison: [12] reports a mean error of 1.8 degrees of arc horizontally, and 3.1 degrees vertically; [13] reports a mean deviation of ±3.3 cm. These ratings serve as a guideline for the design of EOG controlled applications.

The estimation algorithm is defined for any subset of electrodes. Using the recordings described above, we compute the accuracy of the estimation on subsets of electrodes. We investigate which electrodes are most valuable to simultaneously minimize the error in left-right and up-down glance.

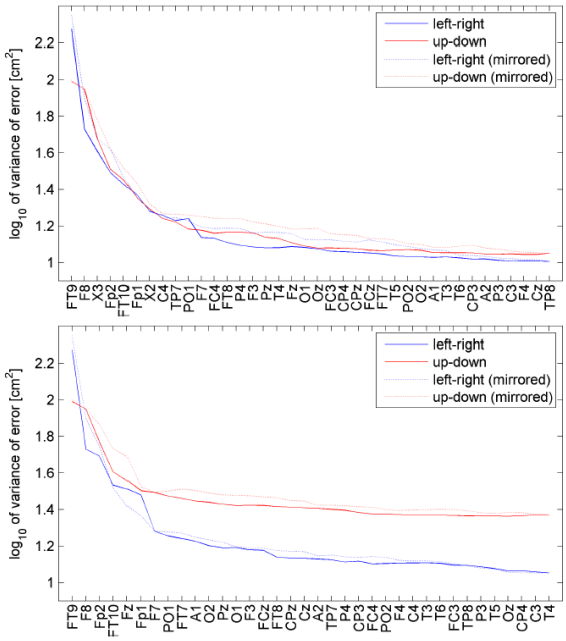

Fig. 4: Ordering of electrodes that minimize the maximum of horizontal and vertical estimation error obtained by greedy optimization. The dashed lines correspond to the ordering of electrodes mirrored along the centerline of the head for the purpose of comparison. *Top:* Electrodes X2 and X3 are connected 2cm below the eyes. *Bottom:* No electrodes below the eyes.

Using greedy optimization, we minimize

$$\sum_{j=1}^{12} \max\{var\ e_j^x(t), var\ e_j^y(t)\} \qquad (5)$$

where $e_j(t)$ denotes the error function for subject $j = 1,2,\ldots,12$: starting with an empty subset of electrodes, each iteration we add the respective electrode that reduces Equation (5) most. This process yields a priority list of electrodes, see Figure 4. For instance, if the system ought to run with nine electrodes only, our evaluation suggests to connect FT9, F8, X3, Fp2, FT10, Fp1, X2, C4, and ground

GND. The configuration may be mirrored along the centre line of the head without loss of precision.

C. Application Benchmarks

Software to spell words is a popular benchmark among applications controlled by EOG [4]. Our spelling software demonstrates the reliability and convenience of our novel drift compensation. The letters of the English alphabet are aligned sequentially along an ellipse on the screen. This alignment increases the probability that an offset in the estimation of glance due to drift resulting in a position outside of the screen, is corrected. In addition, our speller is dictionary based, which generally eases the selection of characters after the first few letters of a word have been spelled. Figure 3 shows the coordinates of $\hat{x}$ and $\widehat{x'}$ for a sample trial. A calibration process of 1 minute duration precedes the spelling.

In a recording of 27 minutes duration 358 characters (including spaces) were spelled. This is equivalent to 13.25 characters per minute with an accuracy of 100%. The average number of characters to choose from was $N = 17.4$, the average duration for a character selection was $T = 4.7$ seconds, and the selection was correct with a probability of $P = 0.98$ (errors could be corrected by a backspace function). In terms of the information rate derived from [14], the number of bits transferred per second was

$$\frac{1}{T}\left(\log_2 N + P\log_2 P + (1-P)\log_2\frac{1-P}{N-1}\right) = 0.83\frac{bits}{s} \quad (6)$$

For comparison: The EOG controlled speller in [4] allows subjects to spell 5 letters in 24.7 sec.

Another application classic is the game *Breakout* [15]: The game is about positioning a paddle on the bottom of the screen to bounce off a ball. The control in our implementation relies only on the correct estimation of x-glance. To create an incentive for the subject to vary the glance along the x-axis and to reach the boundary of the screen, the ball never bounces off vertically. The gameplay consists only of a single state and is intuitive. Playing the game has been the favourite activity among the 12 volunteers who tested our EEG system.

IV. CONCLUSION

Previous EOG-based control schemes applied a high-pass filter to overcome the drift in the voltage measurements. Because the filter removes any constant offset, these schemes allow only for velocity control: rapid eye movements of the subject are recognized, but steady glance is not encoded. Therefore, EOG-based applications typically consist of a set of states. Transitions between the states occur when the subject oscillates the glance direction, or blinks [4]. However, fast oscillation of gaze direction, or frequent eye blinking can cause subject fatigue over a prolonged period. In contrast, our algorithm does not filter the data. The subject controls the application by simply glancing at a target location on a computer screen. As a consequence, our applications use fewer states, and are more seamless to operate. The numerical evaluations and the performance of our benchmark applications suggest that control via glance direction is both more accurate and less exhausting than control via rapid eye gestures. Researchers have custom built EOG circuits, in order to reduce the cost and complexity of hardware [3]. We look forward to learn about applying our algorithm on this specialized hardware. The glance estimation presented in this paper has a smaller calibration-to-operation ratio and is numerically stable. In the future, we hope to show that our algorithm benefits the removal of eye artefacts from EEG.

REFERENCES

[1] R. Barea, L. Boquete, M. Mazo, and E. Lopez, *System for Assisted Mobility Using Eye Movements Based on Electrooculography*, IEEE Transactions on Neural Systems and Rehabilitation Engineering, vol. 10, no. 4, pp. 209-218, 2002

[2] Y. Chen and Y. Newman, *A Human-Robot Interface Based on Electrooculography*, Proceedings of the IEEE International Conference on Robotics and Automation, pp. 243-248, April 2004

[3] S. Venkataramanan, P. Prabhat, S. Choudhury, H. Nemade, and J. Sahambi, *Biomedical Instrumentation based on Electrooculogram Signal Processing and Application to a Hospital Alarm System*, Proceedings of the 2nd IEEE International Conference on Intelligent Sensing and Information Processing, pp. 535-540, January 2005

[4] A. Usakli and S. Gurkan, *Design of a Novel Efficient Human-Computer Interface: An Electrooculagram Based Virtual Keyboard*, IEEE Transactions on Instrumentation and Measurement, vol. 59, no. 8, pp. 2099-2108, August 2010

[5] C. Hsieh, H. Chen and T. Jong, *The Study of the Relationship between Electro-oculogram and the Features of Closed Eye Motion*, Proceedings of the 5th International Conference on Information Technology and Application in Biomedicine, May 2008

[6] M. Fatourechi, A. Bashashati, R. Ward, and G. Birch, *EMG and EOG artefacts in brain computer interface systems: A survey*, Clinical Neurophysiology 118, pp. 480-494, 2007

[7] R. Barea, L. Boquete, M. Mazo, E. Lopez and L. Bergasa, *E.O.G. Guidance of a Wheelchair using Neural Networks*, International Conference on Pattern Recognition, vol. 4, 2000

[8] D. Kumar and E. Poole, *Classification of EOG for Human Computer Interface*, Proceedings of the 2nd Joint IEEE Annual International Conference of the Engineering in Medicine and Biology Jointly with the 24th Annual Conference of the Biomedical Engineering Society, vol. 1, pp. 64-67, October 2002

[9] Y. Kim, N. Doh, Y. Youm, and W. Chung, *Development of Humanmobile Communication System using ElectroOculoGram Signals*, Int'l Conference on Intelligent Robots and Systems, pp. 2160-2165, 2001

[10] J. Hakenberg,W. Lee, T. Tan, A. Mansour, and C. Guan, *A new paradigm to quantify the manifestation of eye movements in the electroencephalogram*, Proceedings of the Engineering and Physical Sciences in Medicine and the Australian Biomedical Engineering Conference, Dec 2010

[11] J. Kierkels, J. Riani and J. Bergmans, *Using an Eye Tracker for Accurate Eye Movement Artefact Correction*, IEEE Transactions on Biomedical Engineering, vol. 54, no 7, 2007

[12] J. Woestenburg, M. Verbaten, and J. Slangen, *Eye-movements in a 2 dimensional plane: a method for calibration and analysis using the vertical and horizontal EOG*, Biological Psychology, vol.18, pp.149-160, Mar 1984

[13] X. Zhang, T. Sugi, X. Wang, and M. Nakamura, *Real-time estimation system of the gaze position based on an electrooculogram*, Artificial Life Robotics, vol. 14, pp. 182-185, 2009

[14] C. Shannon, and W. Weaver, *The Mathematical Theory of Communication*, The University of Illinois Press, 1964

[15] J. Hakenberg, *Applications of the NuAmps Digital EEG Amplifier*, www.hakenberg.de/automation/neuroscan_nuamps.htm, Mar 2011